2011

The Dynamics of Integrate-and-Fire: Mean vs. Variance Modulations and Dependence on Baseline Parameters

Joanna R. Wares
University of Richmond, jwares@richmond.edu

Todd W. Troyer

Recommended Citation

Wares, Joanna R., and Todd W. Troyer. "The Dynamics of Integrate-and-Fire: Mean Versus Variance Modulations and Dependence on Baseline Parameters." *Neural Computation* 23, no. 5 (2011): 1234-247. doi:10.1162/NECO_a_00114.

The Dynamics of Integrate-and-Fire: Mean Versus Variance Modulations and Dependence on Baseline Parameters

Joanna Pressley
j.pressley@vanderbilt.edu
Department of Mathematics, Vanderbilt University, Nashville, TN 37240, U.S.A.

Todd W. Troyer
todd.troyer@utsa.edu
Biology Department, University of Texas at San Antonio, San Antonio TX 78249, U.S.A.

The leaky integrate-and-fire (LIF) is the simplest neuron model that captures the essential properties of neuronal signaling. Yet common intuitions are inadequate to explain basic properties of LIF responses to sinusoidal modulations of the input. Here we examine responses to low- and moderate-frequency modulations of both the mean and variance of the input current and quantify how these responses depend on baseline parameters. Across parameters, responses to modulations in the mean current are low pass, approaching zero in the limit of high frequencies. For very low baseline firing rates, the response cutoff frequency matches that expected from membrane integration. However, the cutoff shows a rapid, supralinear increase with firing rate, with a steeper increase in the case of lower noise. For modulations of the input variance, the gain at high frequency remains finite. Here, we show that the low-frequency responses depend strongly on baseline parameters and derive an analytic condition specifying the parameters at which responses switch from being dominated by low versus high frequencies. Additionally, we show that the resonant responses for variance modulations have properties not expected for common oscillatory resonances: they peak at frequencies higher than the baseline firing rate and persist when oscillatory spiking is disrupted by high noise. Finally, the responses to mean and variance modulations are shown to have a complementary dependence on baseline parameters at higher frequencies, resulting in responses to modulations of Poisson input rates that are independent of baseline input statistics.

1 Introduction

A fundamental problem in neuroscience is to understand how the functional response properties of neurons depend on the underlying mechanistic parameters at the level of membrane biophysics. To make things more

Neural Computation **23, 1234–1247** (2011)

tractable, the problem of neuronal signaling is often conceptually divided into two processes: synaptic integration and spike generation. Mechanistically, synaptic integration is often studied by measuring the magnitude and duration of postsynaptic potentials, and spike generation is examined by recording spike trains elicited by a series of current steps. Functionally, extracellular spike responses to external stimuli are often characterized using the linear-nonlinear cascade model (Carandini, Mechler, Leonard, & Movshon, 1996; Chichilnisky, 2001), where the input signal is first passed through a linear synaptic filter, followed by a static nonlinear response function. As tempting as it is to make direct connections between the mechanistic measurements and the functional description, research in simple model neurons has demonstrated that common intuitions can be poor guides for predicting neural responses to a barrage of synaptic input.

Central to this work is the leaky integrate-and-fire (LIF) model, the simplest model that captures the basic properties of integration by a capacitive membrane and spike generation based on a voltage threshold (Lapique, 1907, 2007). A common intuition is that the response time of the LIF should be limited by the response time of the membrane, τ_m. In particular, the response to sinusoidal modulations of the input should approach zero for modulation frequencies that are significantly faster than $1/\tau_m$. However, recent studies have shown that under some circumstances, the LIF model continues to respond, even for modulation frequencies approaching infinity (Brunel, Chance, Fourcaud, & Abbott, 2001; Fourcaud & Brunel, 2002). Furthermore, if one applies a signal with constant mean but a sinusoidally modulated variance, the LIF model can follow the variance changes to arbitrarily high frequencies (Lindner & Schimansky-Geier, 2001). Subsequently, slice recordings have confirmed that cortical neurons can follow rapid modulations in the variance of noisy currents (Silberberg, Bethge, Markram, Pawelzik, & Tsodyks, 2004; Boucsein, Tetzlaff, Meier, Aertsen, & Naundorf, 2009). Follow-up studies in generalized integrate-and-fire types of models have examined how the response at very high frequencies is limited by the dynamics of spike initiation (Naundorf, Geisel, & Wolf, 2005; Fourcaud-Trocme & Brunel, 2005; Khorsand & Chance, 2008; Vilela & Lindner, 2009).

In addition to rate responses that are more rapid than individual postsynaptic potentials, the LIF model possesses other response properties that cannot be explained by a process of synaptic filtering followed by spike initiation. For example, the same LIF model can be made to operate in qualitatively distinct regimes of behavior simply by changing the parameters governing the input statistics (Abeles, 1991; Troyer & Miller, 1997). If the mean input current is large and synaptic noise is small, the voltage is driven monotonically across threshold, and spikes are produced at regular intervals. In this "regular regime," the model acts like an oscillator, displaying resonant behavior for perturbations near its baseline firing frequency (Knight, 1972a). If the mean input is subthreshold and the noise is large,

voltage trajectories follow a random walk, and spike times are irregular (Shadlen & Newsome, 1994).

As a first step toward a deeper understanding of LIF dynamics, we sinusoidally modulated the statistics of the input current, specifically the mean and the variance. We then quantified how several aspects of LIF response depend on baseline input parameters, which were chosen to cover the range of LIF behavior. We find that at very low firing rates, the low-pass cutoff frequency for modulations of the mean current matches that expected from capacitive filtering. However, this limiting frequency increases with greater baseline levels of current, and the increase is more rapid with lower noise. We also find that resonant responses to modulations in the variance of the input current are different from the resonant responses to modulations in the mean, as variance-based resonances persist into the random regime and peak at frequencies greater than baseline firing rates. Finally, we demonstrate that at higher frequencies, the responses to mean and variance modulations have complementary dependence on the baseline parameters, implying that the high-frequency gain in response to Poisson inputs will be similar for neurons operating in the regular and random regimes of behavior.

2 Methods

We investigate the response dynamics of the LIF model,

$$C\frac{dV}{dt} = g_L(V_L - V) + I(t), \tag{2.1}$$

where V is the membrane voltage and $I(t)$ is the time-varying stochastic input current. Model parameters are set at numerically convenient values near the typical range for cortical pyramidal neurons. The membrane time constant $\tau_m (= \frac{C}{g_L})$ is set to 10 msec; membrane resistance R $(= \frac{1}{g_L})$ is set to 100 MΩ, and V_L $(= -70$ mV) is the resting potential. The neuron spikes when the voltage reaches threshold θ $(= -60$ mV), after which the voltage is reset ($V_r = -70$ mV). Thus, it takes 0.1 nA of current to drive the cell to spike. For simplicity, we do not include an absolute refractory period, which contributes little to the dynamics other than to slow the mean firing rate and push the model further toward regular spiking.

2.1 Stochastic Differential Equation. We adopt a diffusion approximation in which the input current, $I(t)$, is decomposed into the mean current, $\mu(t)$, plus fluctuations, $\sigma(t)\eta(t)$, where $\eta(t)$ is a gaussian white noise process. $\mu(t)$ represents the mean charge accumulating per time and has units $pC/\text{msec} = \text{nA}$. $\sigma^2(t)$ measures the variance of the charge accumulating per time and has units $pC^2/\text{msec} = \text{nA}^2\text{msec}$.

Our results are based on the Fokker-Planck (forward Kolmogorov) approach (Ricciardi, 1977; Brunel & Hakim, 1999; Knight, 2000; Lindner & Schimansky-Geier, 2001; Allen, 2003) that tracks the probability density over voltage as a function of time, $\rho(V, t)$. The net flux, or rate of flow $J_V(V, t)$, across a given voltage V can be calculated as

$$J_V(V, t) = -\frac{R^2\sigma^2(t)}{2\tau_m^2}\frac{\partial\rho(V, t)}{\partial V} + \frac{(V_L - V(t)) + R\mu(t)}{\tau_m}\rho(V, t). \tag{2.2}$$

The probability density obeys

$$\tau_m\frac{\partial\rho(V, t)}{\partial t} = \tau_m\frac{-\partial J_V(V, t)}{\partial V} \tag{2.3}$$

$$= \frac{R^2\sigma^2(t)}{2\tau_m}\frac{\partial^2\rho(V, t)}{\partial V^2} - \frac{\partial}{\partial V}[(V_L - V(t)) + R\mu(t)]\rho(V, t). \tag{2.4}$$

The first term on the right-hand side is the diffusion term, which describes how the voltage distribution spreads due to noise, and the second term describes the driving effects of the mean input and leak currents. The firing rate is equal to the probability flux crossing threshold, $r(t) = J_V(\theta, t)$, which is then reinjected at voltage reset. Under the standard diffusion approximation, the density must equal zero at the absorbing boundary at threshold, so the firing rate equation becomes

$$r(t) = J_V(\theta, t) = \frac{R^2\sigma^2(t)}{2\tau_m^2}\left(-\frac{\partial\rho}{\partial V}(\theta, t)\right). \tag{2.5}$$

Note that the firing rate equation is a product of two terms. The first term is proportional to the instantaneous input variance. Since the density is zero at threshold, the second term, $-\partial\rho/\partial V(\theta, t)$, is proportional to the probability that the voltage lies within a small boundary layer near threshold. Letting $B(t)$ denote the probability of being near threshold, the firing rate is proportional to $B(t)$ multiplied by the probability that noise causes the trajectory to "jump" across threshold:

$$r(t) \propto \sigma^2(t)B(t). \tag{2.6}$$

This multiplication is key in understanding the dynamic response of the LIF model to changing inputs.

3 Linear Systems Analysis

We characterize LIF dynamics using a linear systems approach. Conceptually we fix baseline values for the mean and variance of the input

current (μ_0 and σ_0^2, respectively). These lead to a baseline firing rate r_0. We consider two types of input perturbations: sinusoidal modulations in the mean, $\mu(t) = \mu_0 + \mu_1 \cos(2\pi\omega t)$, or sinusoidal modulations in the variance, $\sigma^2(t) = \sigma_0^2 + \sigma_1^2 \cos(2\pi\omega t)$. For each combination of modulation frequency and type of input perturbation, the firing rate is approximated as $r(t) = r_0 + r_1(\omega)\cos(2\pi\omega t + \phi(\omega))$. The value $\phi(\omega)$ is the frequency-dependent phase of the response, and the ratio $g_\mu(\omega) = r_1(\omega)/\mu_1$ or $g_{\sigma^2}(\omega) = r_1(\omega)/\sigma_1^2$ is the frequency-dependent gain. Note that the frequency dependence of both the gain and phase can be captured by a single complex valued function, $f(\omega) = g(\omega)e^{i\phi(\omega)}$.

Since the baseline firing rate r_0 varies widely over the range of parameters μ_0 and σ_0^2, we characterize the response gain as the fractional change in firing rate from baseline, $r_1(\omega)/r_0$, divided by the fractional change in the input, μ_1/μ_0 or σ_1^2/σ_0^2:

$$G_\mu(\omega) = \frac{r_1(\omega)/r_0}{\mu_1/\mu_0}, \quad G_{\sigma^2}(\omega) = \frac{r_1(\omega)/r_0}{\sigma_1^2/\sigma_0^2}. \tag{3.1}$$

Note that the use of normalized gain alters the shape of the gain dependence across baseline parameters but not the shape of each gain curve as a function of frequency.

To cover all regimes of model behavior, we varied the baseline mean input μ_0 between 0.05 nA and 0.25 nA in 0.0125 nA steps, and the baseline variance σ_0^2 between 0.004 nA^2 msec and 0.03 nA^2 msec in steps of 0.001 nA^2msec. Parameter values for the figures were chosen as representatives of relatively low (0.0075 nA^2msec) or high (0.015 nA^2msec) noise variance.

Closed-form expressions have previously been derived for the baseline firing rate (Brunel & Hakim, 1999; Lindner & Schimansky-Geier, 2001) and linear response gain (Brunel et al., 2001; Lindner & Schimansky-Geier, 2001). The firing rate function contains the complementary error function, and the gain functions chosen for use rely on parabolic cylinder functions (Lindner & Schimansky-Geier, 2001), which we approximated numerically (Mathematica, Wolfram Research, Cambridge, MA). We also obtained gain curves through numerical simulations of equation 2.4, and found no significant differences over the range of parameters reported here. All results reported here rely on numerical approximations to the analytic solution.

4 Results

4.1 Modulations of the Mean. The responses to modulations in the mean input current are low-pass, with response gain roughly constant for low frequencies but decaying toward zero at higher frequencies (see Figure 1A). The low gain at high frequencies means that the model is

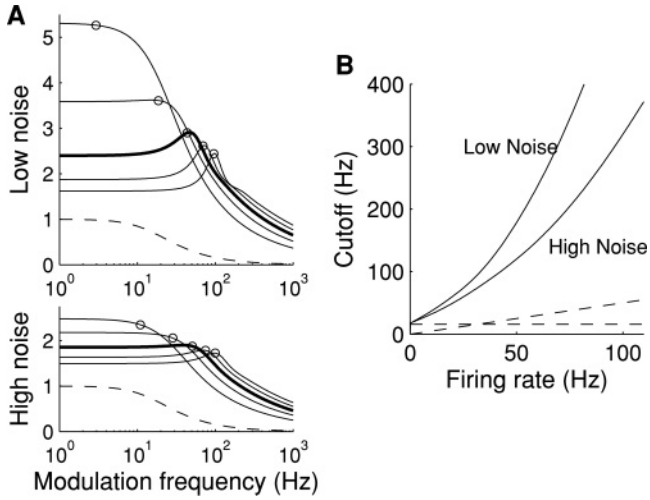

Figure 1: Response gain for modulations in the mean input current. (A) Normalized gain versus frequency for low ($\sigma^2 = 0.0075$ nA^{2}msec, top) and high ($\sigma^2 = 0.015$ nA^{2}msec, bottom) noise. Baseline mean current equals 0.05, 0.075, 0.1, 0.125, and 0.15 nA. The thick middle line represents a just threshold current (0.1 nA); lower currents yield greater low-frequency gain. Circles mark the baseline firing frequency for each set of parameters. The bottom dashed curve shows the gain resulting from the capacitive membrane. (B) Cutoff frequency versus steady-state firing rate for low (top curve) and high (bottom curve) noise. Dashed horizontal line: the cutoff for membrane filtering ($= 1/2\pi\tau_m$); dashed angled line: cutoff expected from Nyquist arguments ($= r_0/2$).

unable to respond rapidly to changes in the mean level of input current. There are two obvious mechanisms that might limit LIF response times. First, responses may be limited by capacitive filtering of the cell membrane. Alternatively, at high rates, spiking and reset can erase past membrane integration at a rate that is faster than the limitations imposed by capacitive filtering. In this case, one might expect the limiting frequency to be near half of the baseline firing frequency, similar to a noiseless integrator that requires two interspike intervals—one short and one longer—to track oscillatory input as it is modulated above and below its mean value (Knight, 1972a, 1972b). This second argument is similar to those governing the Nyquist frequency for digital sampling.

To examine these mechanisms, we calculated the cutoff frequency at which the response power (the square of the response gain) drops to half of the low-frequency limit (see Figure 1B). As in Figure 1A, we fixed the noise at $\sigma_0^2 = 0.0075$ nA^{2}msec or 0.015 nA^{2}msec. The cutoff frequency approaches the membrane cutoff in the limit of very low baseline firing rates

($<< 1\,\text{Hz} = 1/100\tau_\text{m}$) but increases for increasing firing rates. For moderate rates, the cutoff frequency is substantially above the values predicted from membrane filtering ($1/2\pi\tau_m = 15.9$ Hz; dashed horizontal line) or for the perfect integrator ($r_0/2$; dashed angled line) suggesting that the mechanism limiting the response times of the LIF model is distinct from membrane filtering or rate-based sampling. The cutoff frequency is higher for inputs with lower noise versus higher noise, and has a faster than linear dependence on baseline firing rate (Brunel et al., 2001).

For baseline current levels that are supratheshold, the gain curves in Figure 1A show an increase in the response gain for modulations near the baseline firing frequency of the neuron (open circles). These regions of enhanced gain are termed resonances and are common in oscillatory systems driven at their natural frequency (Knight, 1972b). When the noise is large or baseline input is subthreshold, spiking is irregular and firing rate resonances are reduced or absent.

4.2 Modulations of the Variance. The LIF model responds quite differently to modulations in the noise amplitude than it does to modulations in the mean (see Figure 2A). Perhaps the most striking difference is the large gain at high frequencies (Lindner & Schimansky-Geier, 2001). Recall that the firing rate is proportional to the instantaneous variance, $\sigma^2(t)$, times the probability of lying within a boundary layer just below threshold, $B(t)$ (see equation 2.6). At very high frequencies, the integrative membrane filters out changes in the voltage distribution, and $B(t)$ remains essentially constant (Silberberg et al., 2004; Masuda, 2006). As a result, a fractional change in variance leads to the same fractional change in firing rate. Hence,

$$\lim_{\omega\to\infty} G_{\sigma^2}(\omega) = 1. \tag{4.1}$$

This implies that the LIF model is able to respond instantaneously to rapid changes in the input variance.

The plots in Figure 2A reveal that the high-frequency gain increases toward 1 when the mean current is suprathreshold ($\mu_0 > 0.1$ nA), and decreases toward 1 when the mean current is subthreshold. Thus, the division between increasing or decreasing gain for high frequencies corresponds to a common dividing line between the random and regular regimes of LIF behavior.

In the regular regime, the mean return time to threshold depends mostly on the mean input current, and the firing rate is largely independent of the input variance (Salinas & Sejnowski, 2002). As a result, the low-frequency gain is near zero. But in the random regime, increasing the variance substantially increases the probability of a random threshold crossing, and the low-frequency gain is finite, exceeding the high-frequency gain for baseline parameters far into the random regime (see Figure 2A).

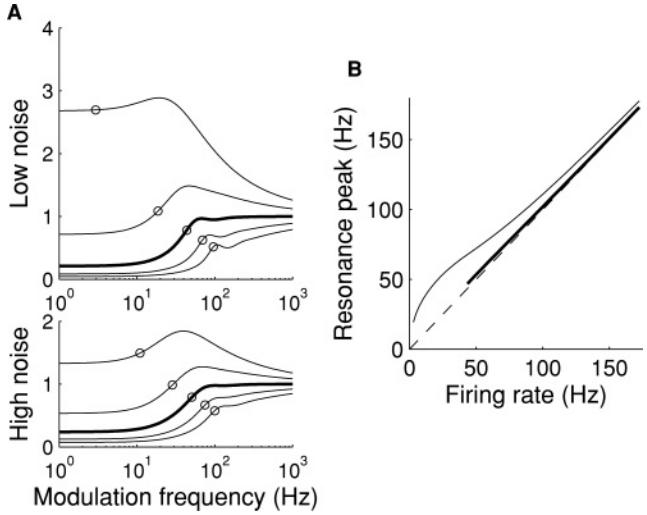

Figure 2: (A) Response gain for modulations in the variance of the input current. Normalized gain versus frequency. Baseline values as in Figure 1. (B) Frequency difference between resonance peak frequency and steady-state firing rate for modulations of the mean (thick, along the diagonal) and variance (thin) for low noise ($\sigma_0^2 = 0.01$ nA^{2}msec). μ_0 ranged from 0.05 to 0.25 nA, leading to firing rates ranging from 3 Hz to 173 Hz. Mean modulations did not yield robust resonances for subthreshold currents ($\mu_0 < 0.1$ nA, firing rate <43 Hz not shown).

To further understand the low-frequency gain, we exploited the multiplicative decomposition of the firing rate, $\tilde{r} \propto \sigma^2 \tilde{B}$ (see equation 2.6), where $\tilde{r}$ and $\tilde{B}$ represent steady-state values of the firing rate and the probability that a trajectory is near threshold for a fixed value of the variance σ^2. Taking derivatives,

$$\frac{\partial \tilde{r}}{\partial \sigma^2}(\sigma^2) \propto \tilde{B} + \sigma^2 \frac{\partial \tilde{B}}{\partial \sigma^2} \tag{4.2}$$

$$\lim_{\omega \to 0} G_{\sigma^2}(\omega) = 1 + \frac{R^2 \sigma_0^4}{2\tau_m^2 \tilde{r}(\sigma_0^2)} \frac{\partial \tilde{B}}{\partial \sigma^2}(\sigma_0^2). \tag{4.3}$$

Since the high-frequency gain is equal to 1, we concluded that the low-frequency gain is larger than the high-frequency gain when $\partial \tilde{B}/\partial \sigma^2 > 0$, and vice versa.

To interpret this result, consider a model subject to a slow increase in the variance. In the regular regime, the drift toward threshold dominates, and changing the variance has little effect on the flow of trajectories entering the subthreshold boundary layer. However, increasing the variance does

cause an increase in the rate that trajectories cross threshold. This decreases the probability of finding a trajectory near threshold, so $\partial \tilde{B}/\partial \sigma^2 < 0$. In the random regime, an increase in variance will cause the steady-state voltage distribution to widen, as well as cause an increase in the probability of leaving the boundary layer. If the spread of the distribution into the subthreshold boundary layer is greater than the increased flow out, then the density in the boundary layer will increase: $\partial \tilde{B}/\partial \sigma^2 > 0$. The point at which the low-frequency gain equals the high-frequency gain corresponds to the point at which the density in the boundary layer becomes more sensitive to the dynamics of subthreshold integration than to the dynamics of spike initiation.

Perturbations in the variance also lead to firing rate resonances, in which response gain is amplified over a relatively narrow range of frequencies (Lindner & Schimansky-Geier, 2001). For the mean, firing rate resonances are found only in the regular regime, and the frequency of peak gain closely tracks the baseline oscillation frequency (i.e., the firing rate; see Figure 2B, thick line). However for modulations in the variance, these resonances persist into the random regime, and the peak frequency is consistently higher than the baseline firing rate (see Figure 2B, thin line). Far into the random regime, the resonance peaks appear to become decoupled from the baseline firing rates, with the baseline firing rates (marked by circles in Figure 2A) falling outside the region of enhanced gain.

4.3 Poisson Input. Thus far, we have analyzed the firing rate response of the LIF model to perturbations of the mean and variance of the input current. However, under the assumption that neurons transmit information through firing rates, the key transformation is from input firing rate to output firing rate. If we assume that the input comes from a single Poisson distributed spike train, then the mean and variance of the input current are proportional: $\mu(t) = Q\lambda(t)$ and $\sigma^2(t) = Q^2\lambda(t)$, where Q is the total charge carried by one input and $\lambda(t)$ is the average rate of the Poisson process. For any combination of baseline mean and variance, we can find a Poisson process generating those statistics by choosing $Q = \sigma_0^2/\mu_0$ and $\lambda_0 = \mu_0/Q$.

Given these values, modulating the input rate by a given fraction $f = \lambda(t)/\lambda_0$ will cause the mean and variance of the input current to be modulated by the same fraction f. For small f, the result of perturbing the mean and perturbing the variance will be additive. Therefore, the response of the LIF model to small modulations of Poisson input rates is simply the sum of the responses to mean and variance modulations, where the addition is applied to the complex valued filter function that encompasses both gain and phase (see section 3). For frequencies greater than the inverse of the membrane time constant, the gain curves coalesce into a common trajectory that drops toward a gain of one (see Figure 3). This implies that the LIF model responds similarly to high-frequency modulations in Poisson input rate, independent of whether the model is operating in the random

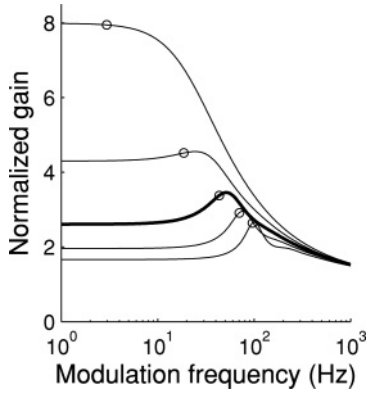

Figure 3: Response gain for modulations of the Poisson input rate. Parameter values as in Figure 1A, top (low noise). The curves converge at frequencies $>1/\tau_m$.

or regular regime of firing. It also implies that although the gain curves for mean modulations and variance modulations are strongly dependent on baseline input parameters (see Figures 1A and 2A), these dependencies are complementary, canceling when the two gain functions are added together. This complementarity does not hold for lower-frequency perturbations, where the response gain for all three types of input modulations—mean, variance, and Poisson rate—is highly dependent on the baseline regime of LIF behavior.

5 Discussion

With the aim of gaining a deeper understanding of LIF dynamics, we quantitatively examined several aspects of LIF responses to sinusoidal modulations in the mean and variance of the input current and how these depend on baseline parameters. In accord with previous studies, LIF responses are low pass in response to modulations in the mean input current. The cutoff frequency approaches that of the membrane filter in the limit of low firing rates, increasing rapidly as the baseline firing rate is increased. This increase is greater with lower noise.

The LIF model also responds to modulations in the variance of the input current, having identical normalized gain at high frequencies in both the regular and random firing regimes. In contrast, the low-frequency gain is highly dependent on regime. Starting from zero in the regular regime, the low-frequency gain increases and then surpasses the high-frequency gain as the mean current is lowered below threshold. The switching point, where low-frequency gain exceeds the gain at high frequencies, comes at the point where the contribution from the variance-induced spread in the overall distribution of voltages begins to play a dominant role in determining the density near threshold (see equation 4.3).

By comparing the gain curves for mean and variance modulations, we have demonstrated that these gain curves have a complementary dependence on baseline parameters at high frequencies. This complementarity implies that in an LIF model driven by a single Poisson input train, the gain function relating high-frequency modulations in Poisson input rate to output spike probability is similar for models operating in the regular and random regimes of spiking (see Figure 3). Previously we have shown that in the perfect integrate-and-fire model (without leak), this complementarity is exact and covers all frequencies: low-pass responses to perturbations in the mean are exactly complementary to high-pass responses to perturbations in the variance, so that responses to Poisson inputs have a uniform gain of one (Pressley & Troyer, 2009).

We speculate that the high-frequency response properties of integrate-and-fire-like neurons, including response complementarity, are dominated by the probability density dynamics within the boundary layer just below spike threshold. Across models, responses are determined by a generalized version of equation 2.6, with firing rates proportional to the probability of being near threshold multiplied the probability of crossing threshold conditioned on the voltage already being near threshold (Troyer, 2006; Helias, Deger, Diesmann, & Rotter, 2010). At very high modulation frequencies, the distribution of voltages does not have time to change (Silberberg et al., 2004; Masuda, 2006), and responses are determined by the probability that trajectories already near threshold go on to produce an action potential. For models where synaptic noise has a finite correlation time, changes in the mean current, as well as changes in the input variance, contribute to the conditional probability of crossing threshold (Fourcaud & Brunel, 2002), resulting in a finite gain in response to high-frequency modulations of the mean input current (Brunel et al., 2001). For models in which the LIF assumption of instantaneous spike initiation is relaxed by including nonlinear voltage-dependent currents (Fourcaud-Trocme, Hansel, van Vreeswijk, & Brunel, 2003; Gutkin & Ermentrout, 1998), spikes take a millisecond or so to initiate, and responses to very high-frequency modulations are filtered out (Naundorf et al., 2005; Fourcaud-Trocme and Brunel, 2005).

If noninstantaneous spiking is included in models expected to have finite high-frequency responses (either variance modulations or mean modulations with correlated noise), one expects gain curves to be qualitatively similar to Figure 1A: low pass with a cutoff that is substantially higher than expected from membrane integration. However, the dynamic mechanisms in the two cases are substantially different, with cutoff frequencies for models with finite spike times in the range of several hundred Hz (Naundorf et al., 2005; Fourcaud-Trocme & Brunel, 2005). At this point, it is unclear whether the cutoff frequencies in the ranges of tens of Hz, for the basic LIF model, are chiefly due to dynamics near threshold or result from more global dynamics having to do with integration and spike reset.

Consistent with previous studies, we found that the LIF model displays response resonances—regions of enhanced gain around a relatively

narrow range of moderate frequencies (Knight, 1972b; Lindner & Schimansky-Geier, 2001). Such resonances are commonly found when oscillatory systems are driven at their natural frequency. Consistent with this notion, resonances for modulations in the mean are found only in the oscillatory regular firing regime, and the peak resonance frequency is very close to the baseline firing rate. In contrast, the peak frequencies of resonances for modulations in the variance persist into the random regime and are significantly greater than the underlying baseline firing rates (see Figure 2B). In both cases, the enhanced gain is likely to result from a dynamic interaction between the processes of synaptic integration and spike initiation. As a result, these effects cannot be easily captured in the cascade description, where the two processes are separated, nor will they be understood by focusing exclusively on the dynamics near spike threshold.

Spurred by results obtained in simple models, several in vitro studies have investigated cortical response properties by injecting noisy currents designed to mimic in vivo patterns of synaptic input. Early studies used stationary statistics and focused on determining the shape of the steady-state response function (Chance, Abbott, & Reyes, 2002; Fellous, Rudolph, Destexhe, & Sejnowski, 2003; Rauch, La Camera, Luscher, Senn, & Fusi, 2003; Giugliano, Darbon, Arsiero, Luscher, & Streit, 2004; La Camera et al., 2006; Arsiero, Luscher, Lundstrom, & Giugliano, 2007). More recently, this approach has been used to investigate step changes (Silberberg et al., 2004) and sinusoidal modulations (Kondgen et al., 2008; Boucsein et al., 2009) of the input current statistics. While there is general agreement between theory and experiment, the point-neuron models considered cannot be expected to match the complexity of real neuronal responses. However, simple models can reveal robust qualitative relationships between input and neuronal parameters and the resulting magnitude of neuronal response. These relationships are most likely to be understood by quantifying responses to systematic changes in input parameters, such as those considered here. Lacking a deeper understanding of simple models, such as the LIF, it will be difficult to determine if the complex dynamics of real neurons stem from greater biological detail or follow directly from the basic dynamics of integrate, fire, and reset.

References

Abeles, M. (1991). *Corticonics: Neural circuits of the cerebral cortex*. Cambridge: Cambridge University Press.

Allen, L. J. S. (2003). *An introduction to stochastic processes with applications to biology*. Upper Saddle River, NJ: Pearson Prentice Hall.

Arsiero, M., Luscher, H. R., Lundstrom, B. N., & Giugliano, M. (2007). The impact of input fluctuations on the frequency-current relationships of layer 5 pyramidal neurons in the rat medial prefrontal cortex. *Journal of Neuroscience, 27*(12), 3274–3284.

Boucsein, C., Tetzlaff, T., Meier, R., Aertsen, A., & Naundorf, B. (2009). Dynamical response properties of neocortical neuron ensembles: Multiplicative versus additive noise. *Journal of Neuroscience, 29*(4), 1006–1010.

Brunel, N., Chance, F. S., Fourcaud, N., & Abbott, L. F. (2001). Effects of synaptic noise and filtering on the frequency response of spiking neurons. *Physical Review Letters, 86*(10), 2186–2189.

Brunel, N., & Hakim, V. (1999). Fast global oscillations in networks of integrate-and-fire neurons with low firing rates. *Neural Computation, 11*(7), 1621–1671.

Carandini, M., Mechler, F., Leonard, C. S., & Movshon, J. A. (1996). Spike train encoding by regular-spiking cells of the visual cortex. *Journal of Neurophysiology, 76*(5), 3425–3441.

Chance, F. S., Abbott, L. F., & Reyes, A. D. (2002). Gain modulation from background synaptic input. *Neuron, 35*(4), 773–782.

Chichilnisky, E. J. (2001). A simple white noise analysis of neuronal light responses. *Network: Computation in Neural Systems, 12*(2), 199–213.

Fellous, J. M., Rudolph, M., Destexhe, A., & Sejnowski, T. J. (2003). Synaptic background noise controls the input/output characteristics of single cells in an in vitro model of in vivo activity. *Neuroscience, 122*(3), 811–829.

Fourcaud, N., & Brunel, N. (2002). Dynamics of the firing probability of noisy integrate-and-fire neurons. *Neural Computation, 14*(9), 2057–2110.

Fourcaud-Trocme, N., & Brunel, N. (2005). Dynamics of the instantaneous firing rate in response to changes in input statistics. *Journal of Computational Neuroscience, 18*(3), 311–321.

Fourcaud-Trocme, N., Hansel, D., van Vreeswijk, C., & Brunel, N. (2003). How spike generation mechanisms determine the neuronal response to fluctuating inputs. *Journal of Neuroscience, 23*(37), 11628–11640.

Giugliano, M., Darbon, P., Arsiero, M., Luscher, H. R., & Streit, J. (2004). Single-neuron discharge properties and network activity in dissociated cultures of neocortex. *Journal of Neurophysiology, 92*(2), 977–996.

Gutkin, B. S., & Ermentrout, G. B. (1998). Dynamics of membrane excitability determine interspike interval variability, A link between spike generation mechanisms and cortical spike train statistics. *Neural Computation, 10*(5), 1047–1065.

Helias, M., Deger, M., Diesmann, M., & Rotter, S. (2010). Equilibrium and response properties of the integrate-and-fire neuron in discrete time. *Front. Comput. Neurosci., 3*, 29.

Khorsand, P., & Chance, F. (2008). Transient responses to rapid changes in mean and variance in spiking models. *PloS One, 3*(11), e3786.

Knight, B. W. (1972a). Dynamics of encoding in a population of neurons. *Journal of General Physiology, 59*(6), 734–766.

Knight, B. W. (1972b). Relationship between firing rate of a single neuron and level of activity in a population of neurons: Experimental evidence for resonant enhancement in population response. *Journal of General Physiology, 59*(6), 767–778.

Knight, B. W. (2000). Dynamics of encoding in neuron populations: Some general mathematical features. *Neural Computation, 12*(3), 473–518.

Kondgen, H., Giesler, C., Fusi, S., Wang, X. J., Luscher, H. R., & Giugliano, M. (2008). The dynamical response properties of neocortical neurons to temporally modulated noisy inputs in vitro. *Cerebral Cortex, 18*(9), 2086–2097.

La Camera, G., Rauch, A., Thurbon, D., Luscher, H. R., Senn, W., & Fusi, S. (2006). Multiple time scales of temporal response in pyramidal and fast spiking cortical neurons. *Journal of Neurophysiology, 96*(6), 3448–3464.

Lapique, L. (1907). Recherches quantitatives sur l'excitation éléctrique des nerfs traitée comme une polarization. *J. Physiol. Pathol. Gen., 9*, 620–635.

Lapique, L. (2007). Quantitative investigations of electrical nerve excitation treated as polarization. *Biological Cybernetics, 97*, 341–349.

Lindner, B., & Schimansky-Geier, L. (2001). Transmission of noise coded versus additive signals through a neuronal ensemble. *Physical Review Letters, 86*(14), 2934–2937.

Masuda, N. (2006). Simultaneous rate-synchrony codes in populations of spiking neurons. *Neural Computation, 18*(1), 45–59.

Naundorf, B., Geisel, T., & Wolf, F. (2005). Action potential onset dynamics and the response speed of neuronal populations. *Journal of Computational Neuroscience, 18*(3), 297–309.

Pressley, J., & Troyer, T. W. (2009). Complementary responses to mean and variance modulations in the perfect integrate-and-fire model. *Biological Cybernetics, 101*(1), 63–70.

Rauch, A., La Camera, G., Luscher, H. R., Senn, W., & Fusi, S. (2003). Neocortical pyramidal cells respond as integrate-and-fire neurons to in vivo-like input currents. *Journal of Neurophysiology, 90*(3), 1598–1612.

Ricciardi, L. (1977). *Lecture notes in biomathematics*. Heidelberg: Springer-Verlag.

Salinas, E., & Sejnowski, T. J. (2002). Integrate-and-fire neurons driven by correlated stochastic input. *Neural Computation, 14*(9), 2111–2155.

Shadlen, M. N., & Newsome, W. T. (1994). Noise, neural codes and cortical organization. *Current Opinion in Neurobiology, 4*(4), 569–579.

Silberberg, G., Bethge, M., Markram, H., Pawelzik, K., & Tsodyks, M. (2004). Dynamics of population rate codes in ensembles of neocortical neurons. *Journal of Neurophysiology, 91*(2), 704–709.

Troyer, T. W. (2006). Factors affecting phase synchronization in integrate-and-fire oscillators. *Journal of Computational Neuroscience, 20*(2), 191–200.

Troyer, T. W., & Miller, K. D. (1997). Physiological gain leads to high ISI variability in a simple model of a cortical regular spiking cell. *Neural Computation, 9*(5), 971–983.

Vilela, R. D., & Lindner, B. (2009). Comparative study of different integrate-and-fire neurons: Spontaneous activity, dynamical response, and stimulus-induced correlation. *Physical Review E, 80*(3), 031909.

Received May 19, 2010; accepted October 7, 2010.